OBSERVATIONS OF SOLAR TYPE II BURSTS AT FREQUENCIES 10–30 MHz

V. N. MEL'NIK[1], A. A. KONOVALENKO[1], H. O. RUCKER[2], A. A. STANISLAVSKY[1], E. P. ABRANIN[1], A. LECACHEUX[3], G. MANN[4], A. WARMUTH[4], V.V. ZAITSEV[5], M. Y. BOUDJADA[2], V. V. DOROVSKII[1], V. V. ZAHARENKO[1], V. N. LISACHENKO[1] and C. ROSOLEN[3]

[1]*Institute of Radio Astronomy, 4, Chervonopraporna St., Kharkov, 61002 Ukraine (e-mail: melnik@ira.kharkov.ua, alexstan@ira.kharkov.ua)*

[2]*Space Research Institute, Austrian Academy of Sciences, Schmiedlstrasse 6, A-8042, Graz, Austria*

[3]*Departement de Radioastronomie CNRS UMR 8644, Observatoire de Paris, France*

[4]*Astrophysical Institute Potsdam, Ander Sterwarbe 16, D-14482 Potsdam, Germany*

[5]*Institute of Applied Physics RAS, 603600 Nizhny Novgorod, Russia*

(Received 14 February 2004; accepted 30 March 2004)

Abstract. We present the results of radio telescope UTR-2 observations of solar Type II radio bursts in the 10–30 MHz frequency range. These events possess a fine structure consisting of fast drift sub-bursts similar to Type III bursts. The frequency drift rate of the Type II bursts at decameter wavelengths is smaller than 0.1 MHz s^{-1}. One of these bursts with herringbone structure has a wave-like backbone that almost does not drift. The features of the observed bursts are discussed.

1. Introduction

Solar Type II radio bursts are associated with shock waves traveling through the solar corona. Wild and McCready (1950) first reported observations of these bursts. Such shock waves can be created by flares or/and coronal mass ejections (Nelson and Melrose, 1985; Classen *et al.*, 1998; Classen and Aurass, 2002). When coronal shock waves propagate into interplanetary space, they may generate solar Type II bursts observed below 1 MHz (Lengyel-Frey and Stone, 1989). Consequently, solar Type II bursts are observed in a wide frequency band, from meter wavelengths up to kilometer and even more. With the launch of the spacecraft ISEE, *Ulysses* and WIND, the experimental study of these bursts was enlarged in frequency from a few tens of kHz to some MHz. However, it should be noted that till now the solar Type II radio burst ground based observations in the decameter band at frequencies from 10 to 30 MHz are practically (however see Leblanc *et al.*, 1998) still lacking. This situation was connected to the absence of corresponding radio telescopes and adequate back-end facilities. In spite of comparably large intensities of phenomena (>1 s.f.u. $= 10^{-22}$ W m^{-2} Hz) it is very important to use large radio telescopes. It is necessary for increasing both signal-to-noise ratio with the aim of their identification and analysis, and signal-interference ratio because of a lot of interference

Solar Physics **222:** 151–166, 2004.

in the decameter range. Investigations of fine frequency-time features demand also large antennae with high performance, high dynamic range back-ends.

Until recently the radio astronomy observations at the world largest decameter radio telescope UTR-2 have been carried out at a few discrete frequencies. This did not enable to distinguish the solar Type II bursts with confidence. However, recently the facilities of radio telescope UTR-2 have been extended. Now the observations are conducted by means of the DSP (digital spectropolarimeter described in Kleewein, 1997) in the continuous frequency band of 12 MHz and by a 60-channel spectrometer from 10 to 30 MHz. This provides the opportunity to find slow drift bursts and to get their fine frequency–time structure by means of a high spectral resolution with high sensitivity of the corresponding equipment.

The aim of this paper is to present results of the radio telescope UTR-2 observations in which the solar Type II radio bursts have first been recorded at decameter wavelengths. The used radio astronomical instruments are outlined in Section 2. The observations of four individual events are described in Section 3. Although solar Type II bursts have a number of well-known properties noticed in other frequency bands, we have stated differences, yet unobserved until recently. We discuss these differences in Section 4. They can provide new information about the outer solar corona and the near-Sun interplanetary space and clarify properties of the shocks associated with Type II bursts.

2. Radio Telescopes and Associated Equipment

2.1. RADIO TELESCOPE UTR-2

The broadband (10–30 MHz) T-shaped radio telescope UTR-2 (Megn *et al.*, 1978; Braude *et al.*, 1978) consists of two antenna arrays: 'N–S' (1800 m long in the north-to-south direction) and 'W–E' (900 m long in the west-to-east direction). The 'N–S' antenna is composed of two separate arrays. Each array has 720 broadband dipoles (6 rows by 120 dipoles). The 'W–E' antenna includes 6 rows by 100 dipoles. The antenna phasing system is discrete. Its 2×10^6 positions cover the observation sector $\pm 70^\circ$ from zenith. The effective area is 10^5 m^2 for the 'N–S' antenna and 4×10^4 m^2 for the 'W–E' antenna when pointed at the zenith. Multiplication of these antennae patterns provides the resultant pattern, having the appearance of a fan composed of five pencil-shaped beams spaced along declination. The width of each of the five beams is about $25'$ at frequency 25 MHz. The antenna system losses are compensated by a set of antenna amplifiers. High dynamic range and linearity of the amplifiers as well as their optimal distribution along the receiving channel almost eliminate the intermodulation interference (Abranin *et al.*, 1995).

TABLE I
Parameter set of DSP.

Bandwidth of the spectral analysis	12 MHz
Frequency resolution	12 kHz
Time resolution	from 2ms to 1 s
Dynamic range	70 dB
Operation frequency band when operating with UTR-2 radio telescope	10–30 MHz

2.2. RADIOMETERS

After the radio telescope has been equipped with new linear broadband antenna amplifiers it became possible to conduct multi-frequency wide-band observations in the entire operational frequency band (10–30 MHz).

For the purpose of solar observations a 60-channel parallel radio spectrometer has been designed. It has 60 identical frequency channels with bandwidths of 3 to 10 kHz depending on the interference conditions. Central frequencies of each channel are chosen in the range 10–30 MHz according to the observation program. The spectrometer provides time resolution up to 10 ms and sensitivity up to $\approx 10^{-25}$ W m^{-2} Hz^{-1}. The spectrometer accomplishes measurements of various solar burst parameters: flux density, duration, frequency drift rate, spectrum width and burst time profile.

During 1999–2002 the observatories of Grakovo (Ukraine), Graz (Austria) and Nançay (France) have been conducting joint observations of the solar sporadic radio emission. For specified periods of time the new digital spectral polarimeter (DSP), a joint Austrian–French development (Lecacheux *et al.*, 1998) was brought into operation in addition to the multi-channel spectrometer.

The DSP is a two-channel broadband digital receiver designed for processing and registering the signals of cosmic sources. Its main characteristic features are summarized in Table I.

2.3. INSTRUMENT TREMSDORF

The radio-spectral-polarimeter of the Astrophysical Institute Potsdam is located at the Observatory of Solar Radioastronomy in Tremsdorf. It covers a frequency range 40–800 MHz. The instrument is divided into four sub-instruments (sweep spectrometers) in the frequency ranges 40–100 MHz, 100–170 MHz, 200–400 MHz, and 400–800 MHz with a sweep rate of 10 per second. Each sub-instrument contains 256 channels (Mann *et al.*, 1992).

3. Observations

Observations of sporadic solar radio emission at the radio telescope UTR-2 were carried out in May 2001 (by means of DSP) and in summer months of 2002 (with DSP and 60-channel spectrometer). We have detected four events that look like Type II bursts (Nelson and Melrose, 1985).

One event was observed on 11 May 2001 (Figure 1(a)). We see that the burst drifts from 32 MHz to 23 MHz with the rate $df/dt \approx -0.07$ MHz s^{-1}. Its characteristic feature is an irregular cloudy structure with the maximum radio flux $S \approx 2 \times 10^{-21}$ W m^{-2} Hz^{-1} at low frequencies (23 MHz), whereas at higher frequencies (32 MHz) its flux is $S \approx 4.7 \times 10^{-21}$ W m^{-2} Hz^{-1}. The DSP allowed us to distinguish the fine structure of the received burst (Figure 1(b)). It consists of fast drift bursts (constituents) with duration $\Delta t \approx 1$ s and flux $S \approx 5 \times 10^{-21}$ W m^{-2} Hz^{-1}. The values of their drift rates are close enough but not equal (from $df/dt \approx -0.8$ MHz s^{-1} up to $df/dt \approx -2.5$ MHz s^{-1}). Moreover, there are some components (07:10:40–07:10:50 UT and 07:11:20–07:11:40 UT) with positive (from lower to higher frequencies) drift $df/dt \approx 2 - 3$ MHz s^{-1}. The full duration of constituents defines the frequency band of the Type II burst. It equals $\Delta f \approx 1 - 3$ MHz. We can discern also a band splitting at frequencies 24 MHz (7:11:40 UT) and 27 MHz (7:10:50 UT).

On 6 July 2002 a solar Type II burst (Figure 2(a)) was registered at 9:48:00 UT and represented four cloudy bright lanes. They follow one after other at intervals 2–3 min at a fixed frequency (or $\Delta f \approx 5$ MHz in frequency domain at a fixed instant of time). It can be assumed that the first two lanes correspond to band splitting of fundamental emission, and the two others are of band splitting of harmonic ones. The frequency drift of each lane is $df/dt \approx -0.03$ MHz s^{-1}. Their frequency band width is about $\Delta f \approx 2$–3 MHz. In fact, the enhanced brightness regions have the fine structure in the form of fast drifting Type III-like bursts (with rate df/dt being from ≈ -0.6 up to -1.5 MHz s^{-1}) especially distinguishable on the DSP spectra (Figure 2(b)). As in the case of the Type II burst (11 May 2001), the lifetime of these sub-bursts defines the frequency band of bright lane components. The sub-burst flux is $S \approx 10^{-19}$ W m^{-2} Hz^{-1} and comparable with the Type III burst flux (Figure 2(a), at 9:52:00 UT) at the corresponding frequencies.

The herringbone structure is a distinctive property of solar Type II bursts (Dulk and McLean, 1978). On 7 July 2002 (Figure 3) we observed such a Type II burst. It began about 11:43:20 UT and its track could be seen until 12:03:00 UT. The Type II burst has a waving backbone with average drift rate equal approximately zero. The herringbone structure sub-bursts (lifetime $\Delta\tau \approx 5$–6 s) drift with the rate $df/dt \approx 1.5$ MHz s^{-1} towards higher frequencies and with the rate $df/dt \approx -0.5$ MHz s^{-1} to lower frequencies. The maximum flux of the sub-bursts yields $S \approx 3.7 \times 10^{-19}$ W m^{-2} Hz^{-1} at 11:49:20 UT. These sub-bursts cover a frequency band of about 10 MHz. Very likely, we observe the fundamental emission near

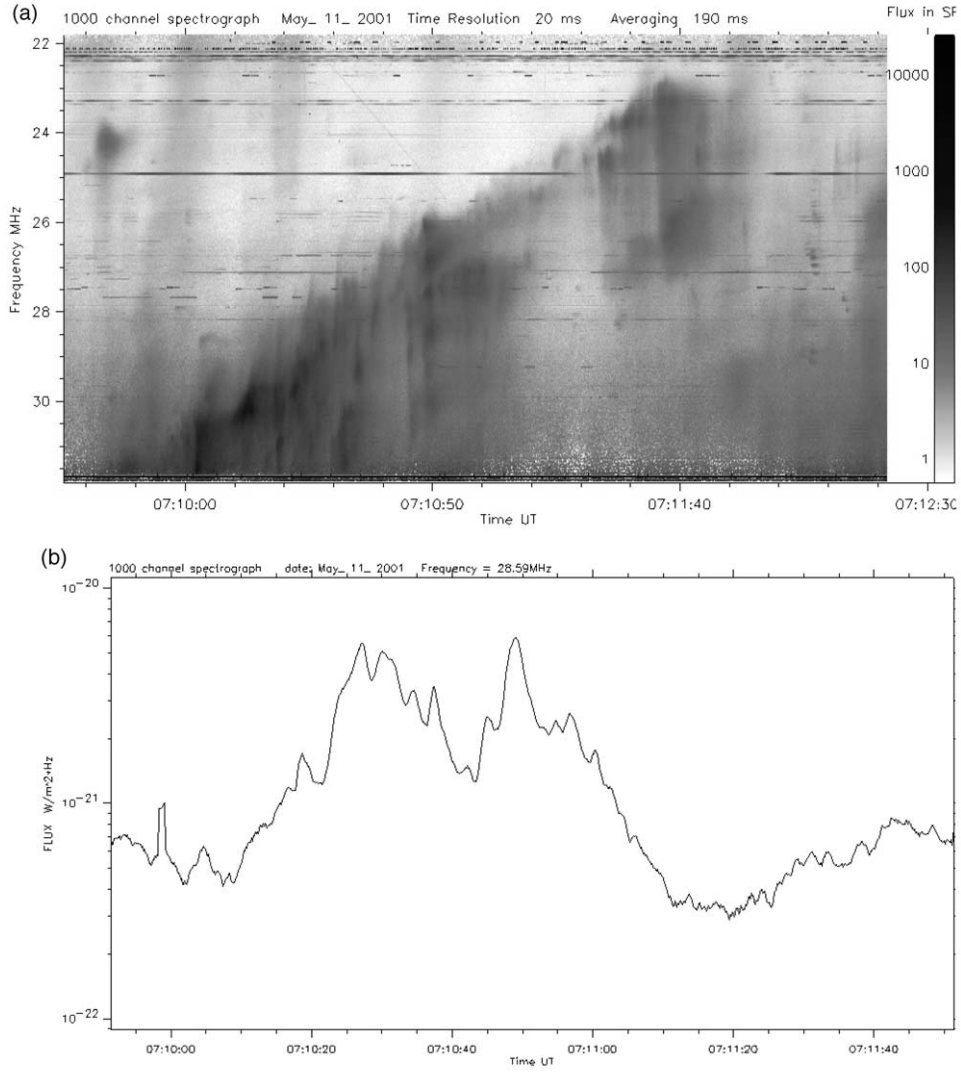

Figure 1. (a) Type II burst as observed by the radio telescope UTR-2 (Kharkov, Ukraine) with DSP (digital spectropolarimeter). Fine structures in the form of Type III-like bursts with positive and negative drifts are seen. (b) The time profile of the Type II burst at frequency 28.59 MHz. The radio emission increasing in flux at 7:10:30 and 7:10:50 UT corresponds to two lanes of the burst.

10 MHz with the radio emission maxima at 11:44:10–11:45:50 UT, 11:46:40–11:50:00 UT and 11:51:40–11:55:50 UT.

An interesting event occurred on 18 July 2002 (Figure 4(a–b)). At 8:21:30 UT a Type II burst with the drift rate $df/dt \approx -0.03$ MHz s^{-1} appeared. In approximately 3 min we observed another Type II-like burst with the drift rate $df/dt \approx -0.05$ MHz s^{-1}. If there were no difference between the drift rates of the two

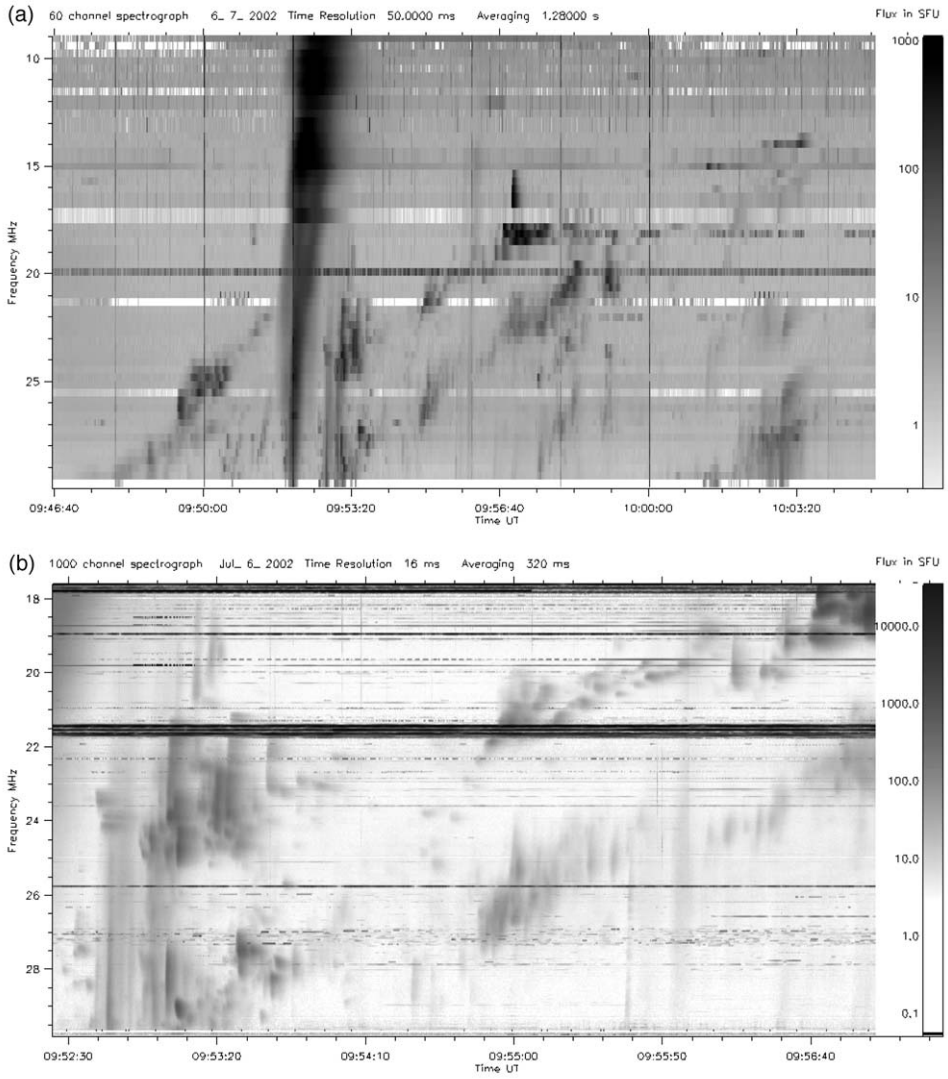

Figure 2. Type II burst with band splitting of fundamental and harmonic emission observed: (a) by 60-channel spectrometer and (b) by DSP. At 09:52:00 UT the Type III burst is visible.

bursts, the second burst could simply be considered as a second lane of band splitting with $\Delta f \approx 3-4$ MHz. However, these two bursts have an appreciable distinction (about a factor of 2) in drift rates. Probably, this is a result of the solar plasma inhomogeneity through which different parts of the shock wave travel. On the other hand, one should not exclude the possibility that their appearance is caused by two independent shock waves traveling simultaneously in the solar corona. As for the 6 July 2002 event the frequency band of each bursts is equal to $\Delta f \approx 2-3$ MHz. Both bursts have a fine structure in the form of Type III-like

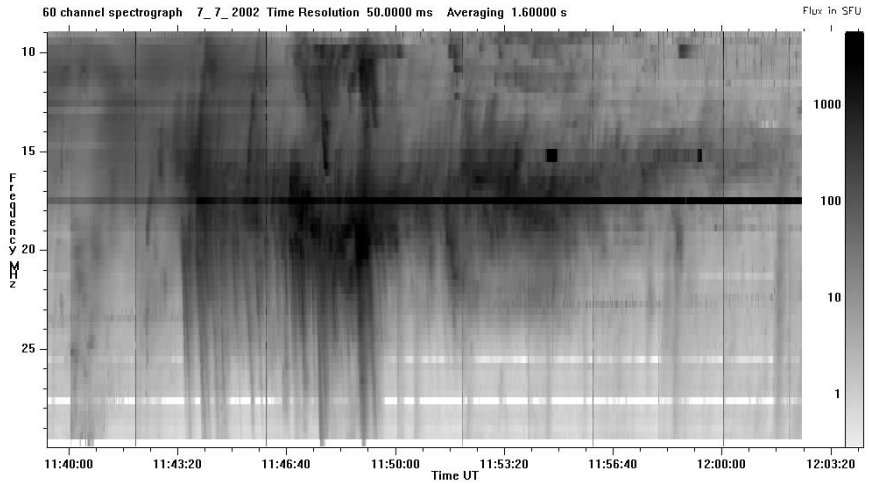

Figure 3. Type II burst with herringbone structure and waving backbone. Fundamental radio emission of this Type II burst is probably visible close to 10 MHz.

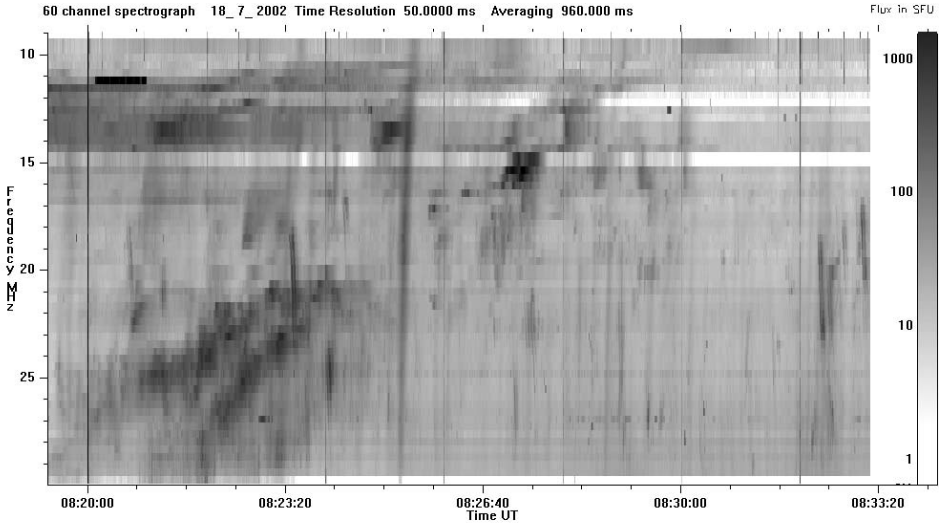

Figure 4a. Band-splitting Type II burst with different frequency drift rates of bands observed by 60-channel spectrometer.

bursts (Figure 4(b-c)) with maximum fluxes of a few $S \approx 10^{-20}$ W m^{-2} Hz^{-1}. These sub-bursts have very large drift rates up to $df/dt \approx -(10 - 15)$ MHz s^{-1} and short duration $\Delta t \approx 1$ s.

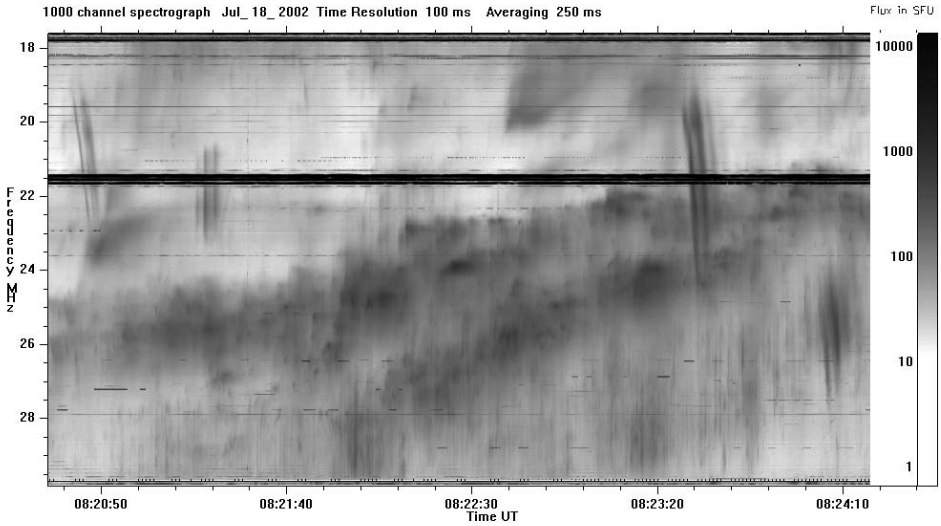

Figure 4b. Band-splitting Type II burst with different frequency drift rates of bands observed by DSP.

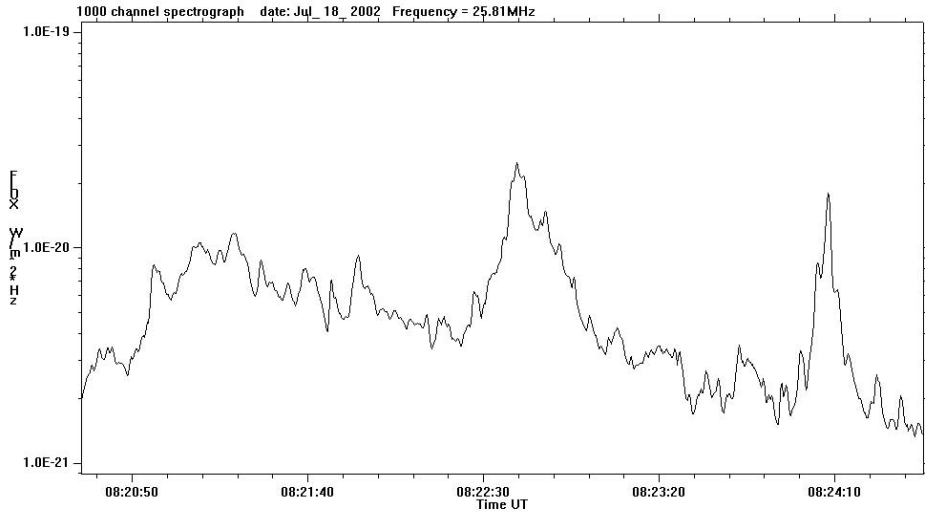

Figure 4c. Time profile of the Type II burst with the fine structure in the form of sub-bursts.

4. Discussion

Decameter Type II bursts as well as the Type II bursts observed in other frequency bands, like meter and kilometer, have frequency drift rates up to hundred times less than those for Type III bursts. Their simultaneous frequency band is sufficiently narrow, 2–10 MHz. The irregular radio emission of such a burst looks like a cloudy structure on a frequency versus time representation. Decameter Type II bursts also

consist of drifting bands with typical frequency splitting $\Delta f/f \approx 0.1$ (Mann, 1995). Both fundamental and harmonic components of Type II bursts are obviously observed in the decameter range. Radio emission flux of the bursts varies between $10-10^3$ s.f.u. These bursts have special features at the decameter radio waves together with the ordinary properties. Below we discuss them in more detail.

Due to the density inhomogeneity of the solar corona the radio radiation which is assumed to be plasma emission, is coming from the outer corona in the frequency range 10–30 MHz. Mann *et al.* (1999) offered a density model of the corona and interplanetary space. It is based on a special solution of the Parker (1958) wind equation and agrees very well with observation from the low corona up to 5 AU. In the outer corona, where the solar wind is very slow, the radial behavior of the electron number density N_e can be expressed by

$$N_e(r) = N_s \exp\left[\frac{A}{R_s}\left(\frac{R_s}{r} - 1\right)\right], \tag{1}$$

with $A = \tilde{\mu} G M_s m_p / k_B T$ ($\tilde{\mu}$, mean molecular weight; G, gravitational constant; M_s, mass of the Sun; m_p, proton mass; k_B, Boltzmann's constant; T, temperature; R_s, solar radius and $N_s = 5.14 \times 10^9$ cm^{-3}). $A/R_s = 13.83$ is found for the temperature of 1.0×10^6 K, which is typical in the outer corona. Then the plasma levels of 30, 20, 10 MHz correspond to radial distances of 1.78, 2.08, 2.94 R_s and from the center of the Sun, respectively. A magnetic field of 0.5 gauss is usually expected in the corona at a distance of $2R_s$ (Mann, 1995), leading to a typical Alfvén speed of 450 km s^{-1} there. Here, the Alfvén speed is defined by $v_A = B/(4\pi\tilde{\mu} N m_p)^{1/2}$, where the full particle number density N is related to the electron number density by $N = 1.92\ N_e$ (B, magnetic field strength). As already mentioned, the radio radiation is generally assumed to be emitted near the local electron plasma frequency $f_{pe} = (e^2 N_e / m_e \pi)^{1/2}$ (e, elementary charge; m_e, electron mass). Then, the drift rate D_f of a signature in a dynamic radio spectrum is related to the velocity of the corresponding radio source V_{source} by

$$D_f = \frac{f}{2}\frac{1}{N}\frac{dN_e}{dr} V_{\text{source}} \times \cos\theta\,, \tag{2}$$

where θ is the deviation angle from the radial direction. Adopting the density model (Equation (1)) in Equation (2), the radial shock speeds ($\cos\theta = 1$) of 880 km s^{-1} and 580 km s^{-1} have been deduced from the drift rates of the events on 11 May 2001 and 6 July 2002, respectively. These speeds are more than CME velocities, 580 km s^{-1} and 280 km s^{-1} (see SOHO/LASCO CME Catalogue, available at *http://cdaw.gsfc.nasa.gov/CME_list/*). It can be understood if harmonic components of Type II bursts were observed in both cases. The 7 July 2002 Type II burst with herringbone structure was accompanied by a fast CME. The latter had velocity 1340 km s^{-1} according to the SOHO/LASCO CME Catalogue. In the event on 18 July 2002 two Type II bursts are superimposed on each other (see Figure 4(a)). Thus, the radial shock speeds of 525 km s^{-1} are 735 km s^{-1} are

found by means of Equation (2) for the lane with the lower and higher drift rates, respectively ($\cos\theta = 1$). In this case CME velocity was also high, 1110 km s^{-1} (from *http://cdaw.gsfc.nasa.gov/CME_list/*). Obviously we observed radio emissions from different CME shock parts, which propagate under some angles to density gradient. As is well known (Dulk, McLean, and Nelson, 1985), in the radial direction (along the plasma's gradient) the shock velocity is higher than in other directions.

4.1. The fine-structure features of decameter Type II bursts

All the observed Type II bursts consist of short bursts with fast frequency drift (some MHz s^{-1}) close to the frequency drift of Type III bursts in the decameter range. Linear velocities of the latter range from $0.1-0.3c$. Taking into account that the duration of Type III-like bursts equals $\Delta t \approx 1$ s, we derive the longitudinal size of electron beams associated with these bursts $\Delta l \approx (3 - 10) \times 10^9$ cm. It is important to emphasize that such fine structures are present not only in the bursts with herringbone structure, but also in the ordinary Type II bursts. They imply that electrons are accelerated on the shocks by *separate* beams (evidently with different velocities judging from the frequency drift rate of sub-bursts) rather than as a whole. Moreover, since the frequency drift rate of the sub-bursts can be both positive and negative, this means that electron beams are moving in different directions off the bow shock, which is propagating away from the Sun.

The presence of two lanes is usually connected with regions on each side of the shock front (Dulk and McLean, 1978). In our case the density jump calculated from the lane frequency splitting should be equal to $\Delta n \approx (1 - 2) \times 10^6$ cm^{-3}. From the above-mentioned observations it follows that sub-bursts have smooth tracks (Figure 1(a)). This means that the beams propagate through plasma with almost uniform density (without any jump). These emission regions are located very probably on one side of the shock wave rather than on different sides (for example, inside a single so-called SLAMS: Short Large Amplitude Magnetic Field Structure, see Classen and Mann, 1998). In this interpretation the cause, why electrons emit in two different plasma regions, remains unclear.

There exists also another significant question, why electron beams disappear to pass these regions. One of several possible explanations of the fact lies in the radio emission conditions of these beams. If the radiation mechanism is believed to be via plasma waves, we can suppose that the level of plasma waves (Langmuir and ion-sound waves) will grow in these regions. They increase the effectiveness of transformation processes of Langmuir waves, generated by electron beams, into transversal waves. The spatial size of regions where electron beams radiate, for the coronal model such as for instance of Mann *et al.*, 1999, is equal to $\approx 0.1\ R_s$.

With regard to the burst with the herringbone structure (7 July 2002), it propagates almost perpendicular to the density gradient. Consequently, the corresponding shock wave is perpendicular. From the backbone width we derive the shock wave

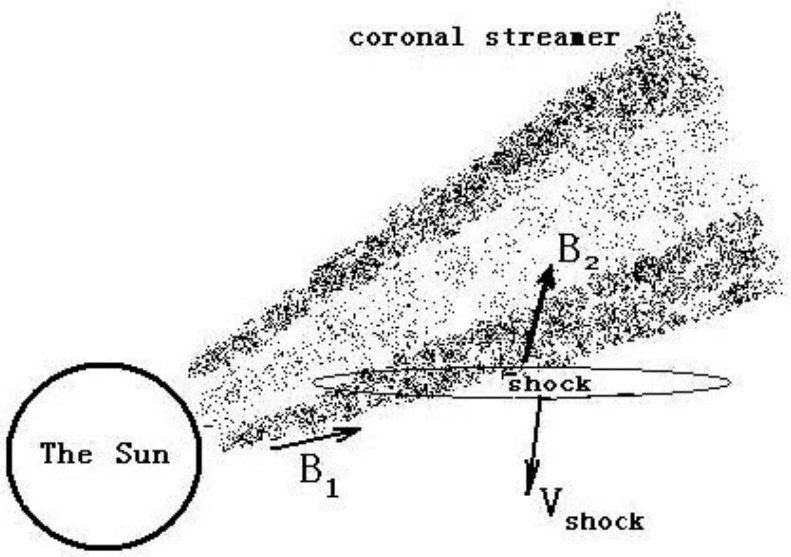

Figure 5. Schematic sketch of shock movement through the solar corona with streamers.

spatial width, $\approx 10^9 - 10^{10}$ cm. If we suggest that electrons are accelerated to the same velocities in both directions towards the Sun and away from the Sun and the non-uniformity of the coronal plasma density is equal on both front sides ($(dn/dr)_{\text{upstream}} \approx (dn/dr)_{\text{downstream}}$), then one of the possible explanations of the differences of drift rates towards higher and lower frequencies observed in the 7 July 2002 event can be connected with electron motion under different angles to the density gradient before and behind shock front that moves with velocity $\mathbf{V}_{\text{shock}}$. It is natural to suppose that before the front (Figure 5) electrons move along a density gradient that coincides with the antiparallel direction of magnetic field lines $\mathbf{B}_1$. Owing to the change of the direction of magnetic field $\mathbf{B}_2$ behind the shock front (Akhiezer, 1974; Zaitsev *et al.*, 1998) electrons move not along the density gradient but magnetic field lines $\mathbf{B}_2$ so drift rates must be smaller, see Equation (2). If this scenario is correct then it gives an opportunity to find the change of magnetic field lines on the shock front proceeding radio data.

4.2. TYPE II BOW-SHOCK INTERSECTION OF THE CORONAL STRUCTURE

Since the Type II burst (7 July 2002) has an almost zero drift rate[1], most likely it is generated by the shock moving perpendicular to the coronal density gradient (angle between $\mathbf{V}_{shock}$ and $\mathbf{B}_1$ is almost 90°). The backbone waving in frequency can be interpreted as an intersection of the coronal structure by the shock. The frequency maxima of the backbone structure correspond to the shock passage through coronal streamers. When we observe frequency minima, the shock moves outside streamers. Assuming that the radio emission is harmonic, the transverse size between streamers equals to 0.3 R_s. Then the streamer width is about 0.1 R_s, and the difference between the streamer density and the density beyond the bounds of the streamer is $\approx 6.3 \times 10^5$ cm^{-3}.

4.3. COMPARISON WITH HIGH-FREQUENCY DATA (TREMSDORF OBSERVATIONS)

Using the Tremsdorf observations, we have tried to find high-frequency precursors of the decameter Type II bursts discussed here. From the decameter data we have derived the linear velocity of shocks associated with the observed Type II bursts (except for the Type II burst of 7 July 2002) applying different models of the solar corona (Newkirk, 1961; Mann, 1995). The value of the velocity is approximately 350–880 km s^{-1}. Correspondingly, the time delay between the decameter Type II bursts and meter wavelengths bursts (for example, 50 MHz) must be about 5–10 min, if the shock velocity does not change during propagation in the low corona. Figure 6 shows the corresponding data of Tremsdorf observations. For the 6 July 2002 event there were precursors at higher frequencies observed during period 9:35–9:45 UT. Unfortunately, for the 18 July 2002 Type II burst, there are no noticeable (or very weak) radio emission structures typical for Type II bursts. In our opinion this may be connected, for example, with radiation beam peculiarities created by shocks. Another explanation may be that a shock, first weak in the low corona (due to $n_{b,s} \approx n_c$, where $n_{b,s}$ is the density behind the bow shock front, n_c is the coronal density), becomes stronger in the course of propagation away from the Sun because the coronal density sharply decreases.

5. Conclusions

Observations of solar decameter Type II bursts, now for the first time recorded by the radio telescope UTR-2, show that these bursts keep the main ordinary properties: slow frequency drift (< 0.1 MHz s^{-1} at decameter wavelengths), narrow simultaneous frequency band of radio emission (2–3 MHz), band-splitting (3–5 MHz

[1]If near its origin the shock wave propagates almost radially, at a long distance the shock front becomes spherical. Thus, there are parts of the shock front moving at right angle to the radial direction. Probably, from them we observed the Type II burst of 7 July 2002.

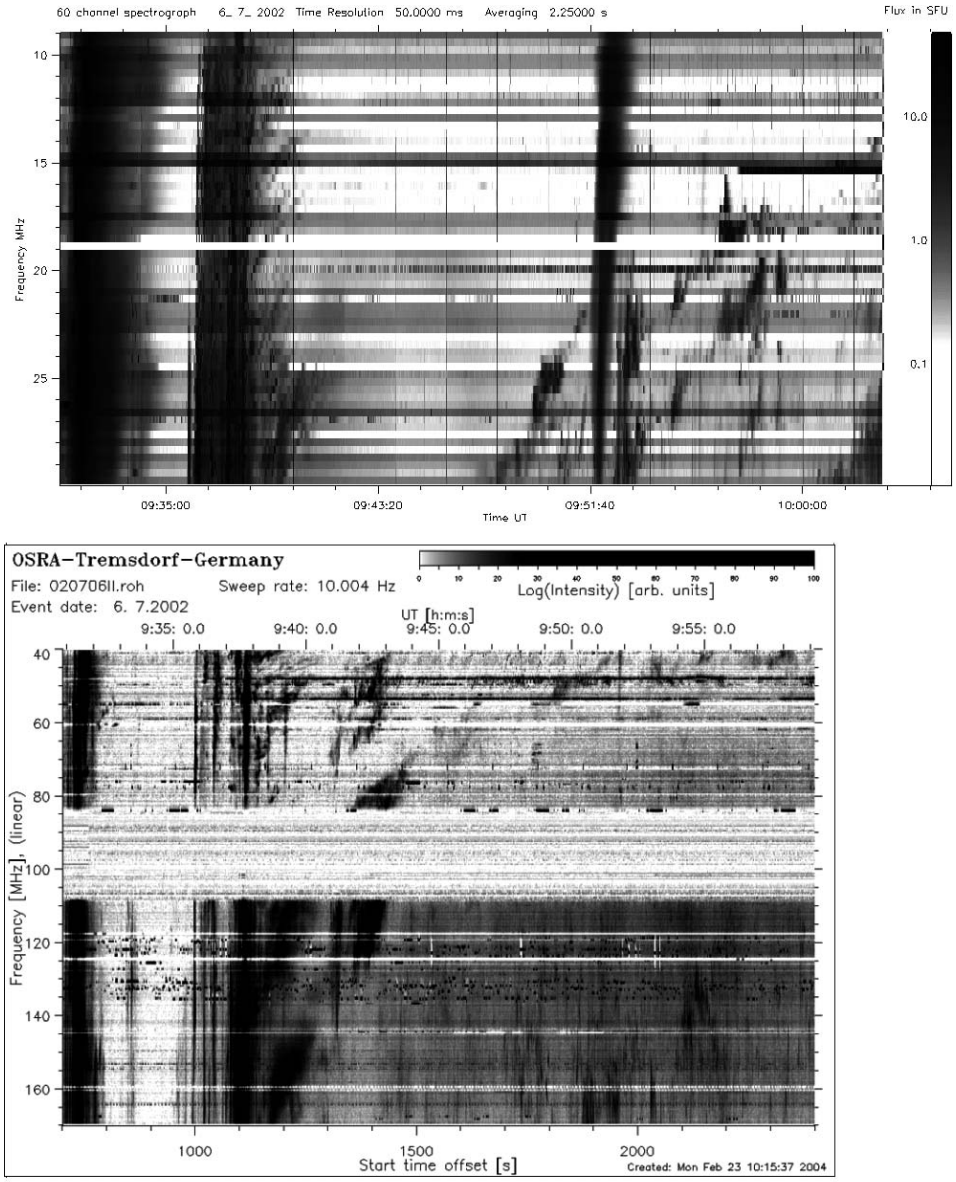

Figure 6a. Observational data from UTR-2 (*above*) and Tremsdorf (*below*) radio telescopes for the event of 6 July 2002.

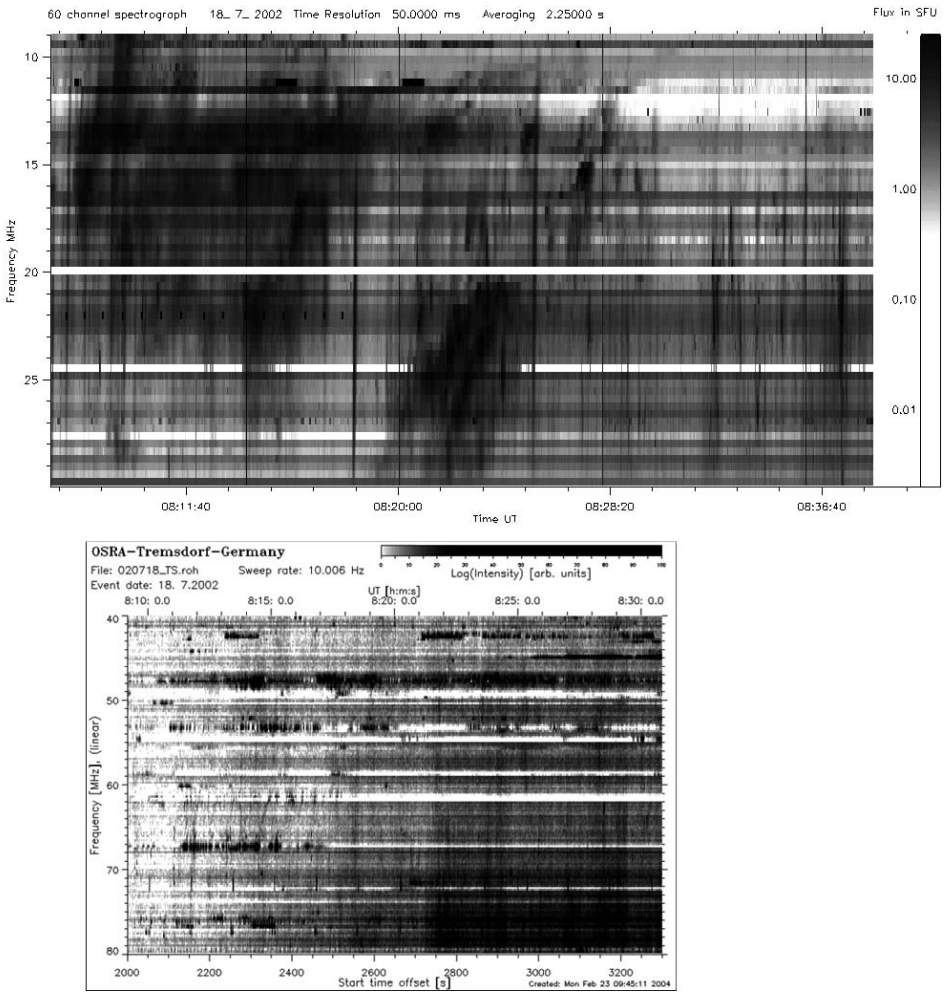

Figure 6b. Observational data from UTR-2 (*above*) and Tremsdorf (*below*) radio telescopes for the event of 18 July 2002.

at decameter range), cloudy structure, herringbone structure, fundamental and harmonic radio emission, high intensity of radio emission (from 10 to 10^3 s.f.u.).

The interesting and important feature of the decameter Type II bursts now visible is that they have a fine structure in the form of Type III-like bursts. The drift rates of these sub-bursts are close to the ordinary Type III bursts velocity, but their duration is essentially lesser. According to our previous results (Abranin, Bazelyan, and Tsybko, 1990), the duration of decameter Type III bursts is about 4–10 s, whereas the duration of sub-bursts is $\approx$ 1 s. Besides, the ordinary Type III bursts propagate at large distances, and sub-bursts cover only $\approx 10^{10}$ cm. According to Suzuki and Dulk (1985), the duration of Type III bursts decreases inversely with frequency. The meter-wave observations show that the duration of type III-like

bursts is 0.2–0.4 s (Slottje, 1981; Zlobec and Thejappa, 1987; Zlobec *et al.*, 1993). Our results reveal that the duration trend (inversely proportional to the frequency) found for type III bursts is valid mainly for type III-like bursts too[2].

From the constant slope of sub-burst tracks (that intersect and form two lanes of increasing radio emission) it follows that these regions seem not to be separated by the shock front with a sharp density drop. The availability of sub-bursts with positive and negative frequency drifts simultaneously shows that electrons are accelerated on the shock in both directions – to the Sun and out of the Sun. In our opinion some increased level of the Langmuir and ion-sound turbulence probably characterizes the band splitting regions. The Type II burst with the herringbone structure is associated with perpendicular shock waves that intersect streamers with a transverse size of 0.1 R_s and an internal density of 6.3×10^5 cm^{-3}.

Acknowledgements

This work was partly realized within the framework of the INTAS project (No. 97-1964) and the INTAS call 2003. We appreciate Prof. P. Zlobec for his useful remarks. V.N.M. thanks the Space Research Institute of the Austrian Academy of Sciences for the hospitality during his visit at Graz.

References

Abranin, E. P., Bazelyan, L. L., and Tsybko, Y. G.: 1990, *Astronomicheskii Zhurnal* **67**, 141.

Abranin, E. P., Bruck, Yu. M., Zakharenko, V. V., and Konovalenko, A. A.: 1995, *Radiofizika i Radioastronomia* **2**, 95.

Akhiezer, A. I.: 1974, *Electrodynamics of plasmas*, Nauka, Moscow, p. 92.

Braude, S. Ya., Zhouck, I. N. , Megn, A. V., Ryabov, B. P., Sharykin, N.K.: 1978, *Astrophys. Space Sci.* **54**, 3.

Classen, H.-T. and Aurass H.: 2002, *Astron. Astrophys.* **384**, 1098.

Classen, H.-T., and Mann, G.: 1998, *Izv. VUZov Radiofizika* **41**, 64.

Classen, H.-T., Aurass, H., Klein, K.-L., Hofmann, A., and Mann, G.: 1998, *Astron. Astrophys.* **343**, 287.

Dulk, G. A. and McLean, D. J.: 1978, *Astron. Astrophys.* **66**, 315.

Dulk, G. A., McLean, D. J., and Nelson, G. J.: 1985, in D. J. McLean and N. R. Labrum (eds.), *Solar Radio Physics*, Cambridge University Press, Cambridge, p. 53.

Kleewein, P., 1997: *Spectral analysis of magnetospheric radio emissions*, Ph. D. Thesis, University of Graz.

Leblanc, Y., Cane, H., Erickson, W. C., Dulk, G. A., and Bougeret, J.-L.: 1998. *Metsaehovi Publications on Radio Science. CESRA Workshop on Coronal Explosive Events, held 9–13 June.* HUT-MET-27, p. 51.

Lecacheux, A., Rosolen, C., Clerc, V., Kleewein, P., Rucker, H. O., Boudjada, M., and Van Driel, W.: 1998, *Low Frequency Radio Astronomy. SPIE Hawaii*. March.

Lengyel-Frey, D. and Stone, R. G. J.: 1989, *Geophys. Res.* **94**, 159.

[2]The fact was drawn to our attention by Prof. P. Zlobec.

Mann, G.: 1995, in: A. O. Benz and A. Kruger (eds.), *Coronal Magnetic Energy Releases*, Springer Verlag, p. 183.

Mann, G., Aurass, H., Voigt, W., and Pashke, J.: 1992, *Proc. First SOHO Workshop, ESA-SP* **348**, 129.

Mann, G., Sansen, F., MacDowall, R. J., Kaiser, M. L., and Stone R. G.: 1999, *Astron. Astrophys.* **348**, 614.

Megn, A. V., Sodin, L. G., Sharykin, N. K., Bruk, Yu. M., Melyanovskii, P. A., Inutin, G. A., and Goncharov, N. Yu.: 1978, *Antenny*, No. 26, Moscow, Svyaz, 15.

Nelson, G. J. and Melrose, D. B.: 1985, in D. J. McLean and N. R. Labrum (eds.), *Solar Radio Physics*, Cambridge University Press, Cambridge, p. 333.

Newkirk, G. A.: 1961, *Astrophys. J.* **133**, 983.

Parker, E. N.: 1958, *Astrophys. J.* **128**, 664.

Slottje, C.: 1981, *Atlas of Fine Structures of Dynamic Spectra of Solar Type IV-dm and Some Type II Radio Bursts*, Publ. of the Netherlands Fundation for Radio Astronomy, Dwingeloo.

Suzuki, S. and Dulk, G. A.: 1985, in D. J. McLean and N. R. Labrum (eds.), *Solar Radio Physics*, Cambridge University Press, Cambridge, p. 289.

Wild, J. P. and McCready, L. L.: 1950, *Austr. J. Sci. Res. Ser.* **A3**, 383.

Zaitsev, V. V., Zlotnik, E. Ya., Mann, G., Aurass, H., and Klassen A.: 1998, *Izv. VUZov Radiofizika* **41**, 164.

Zlobec, P. and Thejappa, G.: 1987, *Hvar. Obs. Bull.* **11**, 111.

Zlobec, P., Messerotti, M., Karlický, M., and Urbarz, H.: 1993, *Solar Phys.* **144**, 373.